



Preparation of main-chain-type and side-chain-type sulfonated poly(ether ether ketone) membranes for direct methanol fuel cell applications

Jie-Cheng Tsai, Chien-Kung Lin*

Department of Chemical Engineering, National Cheng-Kung University, Tainan 70148, Taiwan

ARTICLE INFO

Article history:

Received 21 May 2011

Received in revised form 22 July 2011

Accepted 24 July 2011

Available online 29 July 2011

Keywords:

Side-chain-type

Sulphonation

Sulfonated poly(ether ether ketone)

Proton exchange membrane

Direct methanol fuel cell

ABSTRACT

Novel main-chain-type and side-chain-type sulphonated poly(ether ether ketone)s (MS-SPEEKs) are synthesised by reacting the sulphonic acid groups of pristine SPEEKs with 2-aminoethanesulphonic acid to improve the nano-phase separated morphology of the material. ^1H NMR and FT-IR spectroscopy are employed to determine the structure and composition of main-chain-type and side-chain-type sulphonated polymers. Flexible and tough membranes with reasonable thermal properties are obtained. The MS-SPEEKs show good hydrolytic stability, and water uptake values ranging from 15% to 30% are observed. Compared to Nafion 117[®], the methanol permeability of the MS-SPEEKs is dramatically reduced to $8.83 \times 10^{-8} \text{ cm}^2 \text{ s}^{-1}$ to $3.31 \times 10^{-7} \text{ cm}^2 \text{ s}^{-1}$. The proton conductivity increases with increasing temperature, reaching 0.013–0.182 S cm^{-1} . A maximum power density and open circuit voltage of 115 mW cm^{-2} and 0.830 V are obtained at 80 °C, respectively, which is significantly greater than the values generated with Nafion 117[®]. The introduction of pendent side-chain-type sulphonic acid groups increases the single-cell performance by more than approximately 20%; thus, the lower water diffusivity, methanol permeability, electro-osmotic drag coefficient and high cell performance indicated that MS-SPEEK is a promising candidate for DMFC applications.

© 2011 Elsevier B.V. All rights reserved.

1. Introduction

Direct methanol fuel cells (DMFCs) are considered the ideal fuel cell system because electric power can be produced through the direct conversion of methanol fuel without reforming equipment. Because of the advantages of DMFCs [1,2], such as high energy density, convenient fuel supply, quick start times and instant refueling, DMFCs have been used as mobile and portable power sources for cell phones, notebook computers and other electronic devices [3]. Polymer electrolyte membranes (PEMs) are one of the key components of DMFC systems. Perfluorinated copolymer membranes with pendant sulphonic acid groups, such as the Nafion[®] series from DuPont, are state-of-the-art PEMs due to their high proton conductivity and excellent chemical stability and mechanical properties [4]. However, commercial applications of these membranes are limited due to their high cost, high methanol crossover, and difficult synthesis and processing. In methanol crossover, methanol passes through the PEM and reacts directly at the cathode, reducing the DMFC voltage, poisoning the catalyst and producing mixed potential losses at the cathode [5,6]. Thus, methanol crossover dramatically reduces the overall efficiency of the cell.

To overcome the drawbacks of Nafion[®] membranes, extensive effort has been devoted to decreasing methanol crossover while maintaining high proton conductivity, reducing production costs and simplifying the synthesis of Nafion[®] membranes. Aromatic polymers are a class of high-performance engineering thermoplastic materials that possess high glass transition temperatures, high thermal stability, good mechanical properties and excellent resistance to hydrolysis and oxidation. Sulphonated poly(ether ether ketone)s (SPEEKs) [7–10], sulphonated polyethersulphones (SPESs) [11–13], sulphonated polyimides (SPis) [14,15] and sulphonated poly(benzimidazole) (SPBIs) [16,17] are wholly aromatic polymers that contain sulphonic acid groups along the main polymer chain. Most of these main-chain-type sulphonated polymers can achieve suitable conductivities at high degrees of sulphonation (DS). However, at temperatures greater than the percolation threshold, the requirements of DMFCs cannot be satisfied due to the high water uptake, low mechanical properties, high methanol permeability and poor stability of the membrane-electrode interface [18,19]. Excessive water uptake may be due to the addition of sulphonic acid groups on the main polymer chain [20].

The properties of PEMs are dependent on the molecular structure and nano-phase separated morphology of the polymer. Kreuer [19] reported that main-chain-type sulphonated polymers show less nano-phase separation between hydrophilic sulphonic acid groups and hydrophobic main polymer chains than Nafion[®] membranes, which contain inefficient ionic networks composed of

* Corresponding author. Tel.: +886 6 2757575x62681; fax: +886 6 2344496.
E-mail address: nickel@mail.ncku.edu.tw (C.-K. Lin).

highly branched and dead-end channels. As a result, the cohesion of the hydrophobic parts decreases as the membrane absorbs water. When water uptake is high, the morphology breaks up, resulting in membrane dissolution.

One method of improving nano-phase separation is to separate the hydrophilic sulphonic acid domain from the hydrophobic main chain domain by placing sulphonic acid groups on the pendent side chain to ensure that the membranes have good hydrolytic stability and high conductivity. A variety of side-chain-type sulphonated polymers have been prepared by chemical grafting or post-sulphonation. Jannasch et al. [21–23] synthesised several branched sulphonated polysulphones via lithiation and sulphoalkylation. Okamoto et al. [24–26] and Watanabe et al. [27–29] developed a series of side-chain-type sulphonated polyimides with pendent sulphonated groups and found that the material showed improved hydrolytic stability and high proton conductivity. Guiver et al. [30–32] synthesised comb-shaped poly(arylene ether sulphone)s containing two or four sulphonic acid groups on the side-chain. Na et al. [33–35] used a post-grafting method to form pendent sulphoalkyl groups and produced several flexible and tough side-chain-type sulphonated poly(aryl ether ketone)s containing hydroxyl moieties. The aforementioned polymers possessed sulphonic acid groups on the pendant side chain and were more stable against thermal degradation, hydrolysis and oxidation. However, fuel cell performance data on these materials are relatively scarce.

In the present study, we produced a novel main-chain-type and side-chain-type SPEEK within a single polymer backbone to improve the nano-phase separated morphology. To our knowledge, this is the first time that this novel sulphonation structure has been synthesised on the main and side chain of a single polymer. Pristine SPEEK was prepared from sulphonic acid, and the resulting sulphonic acid groups were reacted with 1,1'-carbonyldiimidazole and grafted with 2-aminoethanesulphonic acid to obtain MS-SPEEK. The flexibility of the side-chain-type sulphonic acid groups allowed for the formation of a well-defined morphology. The properties of the MS-SPEEKs were investigated in detail, and the water uptake, methanol permeability, proton conductivity and cell performance were determined. Compared to Nafion[®] 117, the PEMs showed superior single-cell performance in a DMFC. Thus, the results demonstrated that MS-SPEEK is a promising candidate for DMFCs.

2. Experimental

2.1. Materials and experiments

2.1.1. Materials

All of the reagents were used as received. PEEK 450G Victrex[®] was provided by ICI Corp, and concentrated sulphonic acid (95–98%) was obtained from Aldrich Chemical Corp. 1,1'-carbonyldiimidazole (CDI) and 2-aminoethane sulphonic acid (taurine) were obtained from Alfa Aesar Corp, and *N,N*-dimethylacetamide (DMAc) and methanol were obtained from Mallinckrodt Corp.

2.1.2. Polymer synthesis

PEEK was sulphonated in concentrated sulphuric acid at room temperature under vigorous mechanical stirring for the desired length of time [7–10]. The resulting sulphonated polymer solution was decanted into excess ice-cold water. The precipitated polymer was filtered and washed several times with distilled water until the pH was neutral and was dried under vacuum at 100 °C for 24 h. Subsequently, the SPEEKs were dissolved in DMAc under vigorous mechanical stirring, and CDI was added into the solution. The resulting mixture was stirred at 60 °C for 3 h. The appropriate amount of taurine was added into the solution, and the mixture

was stirred for 2 h to form MS-SPEEK [36], as shown in Scheme 1. Subsequently, the polymer was isolated by precipitation in water, and the acid was removed by washing several times with distilled water until the pH was neutral. The polymer was dried under vacuum at 100 °C for 24 h. In the present study, the DS of the polymers was 47%, 52%, 57%, 62% and 70%, respectively.

2.1.3. Membrane preparation

All MS-SPEEK membranes were prepared by dissolving the sample in DMAc to form a 5% (w/w) solution. Membranes with different degrees of sulphonation were cast by heating and evaporating the solvent from the solution in a glass Petri dish at 120 °C for 3 h. The membranes were obtained by adding deionised water to the surface of the dish and removing the membranes. The thickness of the membranes was controlled at $65 \pm 10 \mu\text{m}$.

2.2. Proton nuclear magnetic resonance (¹H NMR)

MS-SPEEKs were obtained from a solution of DMSO-d₆ (10%, w/v) at room temperature. The ¹H NMR spectra were collected on a Varian Unity 600 spectrometer and a Bruker AMX 600 spectrometer.

2.3. Fourier transform infrared spectroscopy (FT-IR)

An FT-IR spectrometer with an attenuated total reflection (ATR) attachment was used to confirm the presence of functional groups on the membranes. Spectra were obtained with a Bio-Rad FTS-40A spectrometer at a wavelength of 700–4000 cm⁻¹. Each spectrum was the average of 48 scans, with a resolution of 4 cm⁻¹.

2.4. Transmission electron microscopy (TEM)

TEM samples were first stained with silver ions by immersing in AgNO₃ solution for 24 h. Then, the polymers were fully rinsed using water and dried at room temperature. The samples were embedded in epoxy resin and sectioned using a microtome to yield a 50 nm thick sample which was placed on copper grids. The TEM images were determined by Hitachi H-7500.

2.5. Thermogravimetric analysis (TGA)

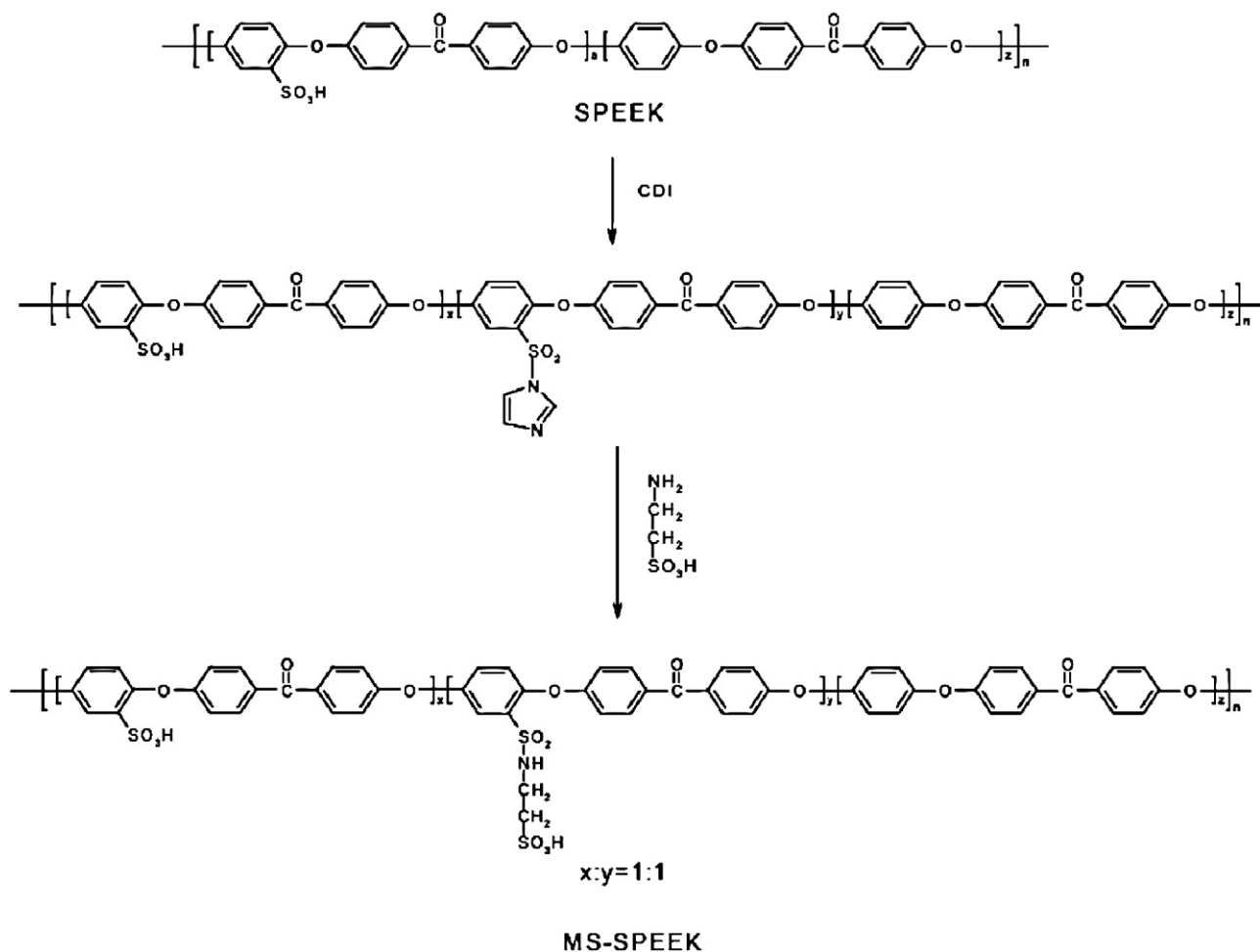
All of the polymers were heated at 100 °C for 30 min in a furnace to remove moisture. Subsequently, dynamic TGA experiments were performed under a nitrogen atmosphere from 100 °C to 800 °C at a heating rate of 20 °C min⁻¹. Thermogravimetric analysis was conducted with a TGA Q50 thermal analyser (TA Instruments, WI).

2.6. Differential scanning calorimetry (DSC)

Thermal analysis was carried out on a DuPont DSC 2910 differential scanning calorimeter from 30 °C to 300 °C at a heating rate of 10 °C min⁻¹ to study the thermal transition behaviour of the polymers. The glass transition temperature (*T_g*) was determined using the second trace of the heating history.

2.7. Liquid uptake of the membranes

Before the equilibrium liquid uptake was measured, the membranes were dried under vacuum at 140 °C until a constant weight was achieved. The equilibrium liquid uptake of the membranes was obtained by immersion in de-ionised water or 2 M methanol solution at 30–80 °C. The amount of liquid absorbed by the polymers was measured at predetermined time intervals until a constant



Scheme 1. The preparation of MS-SPEEK via the post aromatic substitution reaction of SPEEK.

weight was achieved. The weight of absorbed equilibrium liquid was determined according to the following equation:

$$\text{Water uptake (\%)} = \frac{W_{\text{wet}} - W_{\text{dry}}}{W_{\text{dry}}} \times 100\% \quad (1)$$

where W_{wet} and W_{dry} are the weight of the wet and dry membrane, respectively.

2.8. Methanol permeability

The methanol permeability of the membranes was determined using a diaphragm diffusion cell, which consisted of two identical compartments separated by a vertical test membrane. Before the experiment, the membranes were equilibrated in de-ionised water overnight. The initial concentration of methanol in compartment A was 2 M, and compartment B contained deionised water. Throughout the entire permeation experiment, the contents of both compartments were stirred with a magnetic stir bar at room temperature. The change in the concentration of methanol over time in compartment B was determined by gas chromatography. The methanol permeability of the membranes was calculated from the slope of the linear fit to the following equation:

$$C_B(t) = \frac{A}{V_B} \frac{P}{L} C_A(t - t_0) \quad (2)$$

where A is the effective membrane area, L is the membrane thickness, C_A and C_B are the initial concentration of methanol in

compartment A and B, respectively, and V_B is the volume of compartment B.

2.9. Proton conductivity

The proton conductivity of the membranes was determined with an electrochemical cell. Impedance analysis was performed at 30–80 °C with Autolab PGSTAT 30 equipment (Eco Chemie B. V., Netherlands). Frequency response analysis (FRA) software was employed, and an oscillation potential of 10 mV was applied in a thermostatically controlled cell at frequencies ranging from 100 kHz to 10 Hz. The proton conductivity of the membranes was determined according to the following equation:

$$\sigma = \frac{l}{RA} \quad (3)$$

where σ is the proton conductivity, l is the membrane thickness, R is the membrane resistance obtained from impedance analysis, and A is the membrane area.

2.10. Electro-osmotic drag coefficient

Electro-osmotic drag coefficient was measured in the DMFC single-cell test using a known method at 80 °C [37,38]. In order to eliminate any water diffusion across the membrane, cathode humidification was kept by a temperature-controlled water-filled bottle at 80 °C. The anode was supplied with 2 M methanol at a flow rate of 2 mL min⁻¹ with a micropump, and the cathode was sup-

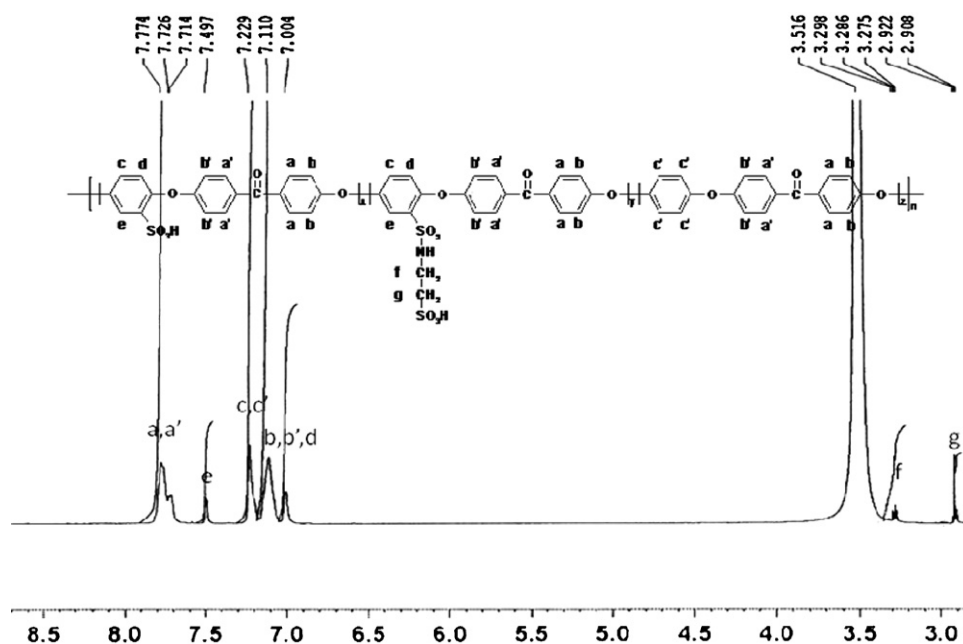


Fig. 1. The ^1H NMR spectra for MS-SPEEK.

plied with O_2 at a rate of 100 mL min^{-1} . Water emerging with the cathode effluent was trapped with anhydrous CaSO_4 . The methanol crossover was calculated from the CO_2 flux in the cathode effluent. The current density from 0 to 500 mA cm^{-2} was produced. Water flux across the membrane was then calculated using the following equation:

$$\text{Water flux across the membrane} = W_T - W_{\text{CH}_3\text{OH}} - W_{\text{current}} - W_{\text{HB}} \quad (4)$$

where W_T , $W_{\text{CH}_3\text{OH}}$, W_{current} and W_{HB} are total water effluent from the cathode exhaust, water from the oxidation of methanol crossover, cell current and the humidity bottle, respectively.

2.11. Single-cell performance

The MS-SPEEKs were investigated as PEMs, and the anode and cathode catalysts were applied to carbon paper by brushing. The anode and cathode consisted of commercial Pt/Ru and Pt with a loading of 3 mg cm^{-2} . The anode was supplied with 2 M methanol at a flow rate of 2 mL min^{-1} with a micropump, and the cathode was supplied with O_2 at a rate of 100 mL min^{-1} . Single-cell performance was evaluated using a DMFC unit with a cross-sectional area of 4 cm^2 .

3. Results and discussion

3.1. Polymer characteristics

^1H NMR spectroscopy was conducted to determine the structure and composition of the MS-SPEEKs. Fig. 1 shows the ^1H NMR spectrum of an MS-SPEEK dissolved in DMSO-d_6 . All of the characteristic peaks of H_a and $H_{a'}$ protons appeared downfield due to the de-shielding effect of the carbonyl group. The H_b protons located at 7.11 ppm were shifted upfield due to the sulphonic groups and the $H_{b'}$ protons located at 7.00 ppm . The $H_{c'}$ protons of the unsubstituted hydroquinone ring appeared as a characteristic singlet at 7.23 ppm . The sulphonic groups were introduced into the hydroquinone ring, which was activated for electrophilic substitution, causing a significant downfield shift of the H_c , H_d , and H_e sig-

nals of the hydroquinone ring. The intensity of the H_e signal at 7.50 ppm , which corresponded to the hydrogen atoms adjacent to the main-chain-type sulphonic acid groups, was equivalent to the sulphonic group content. The DS can be derived from the ratio between the peak area of the H_e signal and the peak area of the other aromatic hydrogen atoms [7,39]. The total DS of sulphonic acid was 0.47 , 0.52 , 0.57 , 0.62 and 0.70 . After introducing pendent side-chain-type sulphonic acid groups, the presence of aliphatic groups resulted in distinct proton signals at 3.29 ppm and 2.91 ppm (H_f and H_g , respectively), indicating that taurin was successfully attached to main-chain-type sulphonic acid groups to form the MS-SPEEK [33–35]. Thus, main-chain-type and side-chain-type sulphonic acid groups were present on the same polymer chain. The degree of side-chain-type substitution was derived from the ratio between the peak area of the H_f signal and the peak area of H_e signals. The ^1H NMR spectroscopy results revealed that the ratio of main-chain-type sulphonic acid groups to side-chain-type sulphonic acid groups was equal to $1:1$. In the present study, the MS-SPEEKs were labelled as MS47, MS52, MS57, MS62 and MS70, respectively.

The FT-IR spectra of SPEEK and MS-SPEEK are shown in Fig. 2. The broad band at $\sim 3460 \text{ cm}^{-1}$ was assigned to the vibration of O–H groups; thus, the sulphonic groups in SPEEK and MS-SPEEK interacted with H_2O . The aromatic C–C band was split into two peaks at 1470 cm^{-1} and 1493 cm^{-1} due to the substitution achieved by sulphonation. The absorption peak at 1022 cm^{-1} , which was assigned to the S=O stretching vibration, was shifted to 1026 cm^{-1} due to the introduction of pendent side-chain-type sulphonic acid groups. The absorption peaks at 1080 cm^{-1} and 1250 cm^{-1} were assigned to the symmetrical O=S=O stretching vibration and asymmetric stretching vibration of sulphonic acid groups, respectively [37]. The absorption peak at 1651 cm^{-1} was assigned to the stretching band of the carbonyl located along the backbone of the polymer chain.

3.2. Morphology of the membranes

The physical and electrochemical properties of PEM should closely relate to the molecular structure and nano-phase separated morphology. The morphology of SPEEK and MS-SPEEK membranes

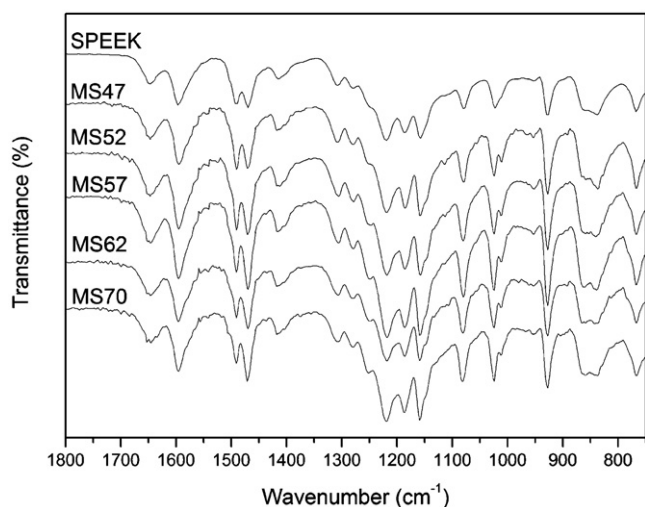


Fig. 2. The FT-IR ATR spectra of SPEEK and MS-SPEEKs.

was investigated by TEM analysis. It has been known that silver ions can chelate with the sulphonic groups, resulting in silver clusters within the polymer matrix. In this study, silver ions were used to observe the morphology of membranes. Fig. 3 shows the TEM images of SPEEK and MS-SPEEK that the sulphonic groups might aggregate into hydrophilic clusters. The darker regions represent hydrophilic ionic domains which could provide proton transport pathways or ionic transport channels while the brighter regions refer to hydrophobic domains. The darker clusters were randomly dispersed throughout the hydrophobic polymer matrix. The ionic clusters, respectively, showed approximate sizes of 2.7 and 4.9 nm for the membrane of SPEEK and MS-SPEEK. It was found that the MS-SPEEK membranes had larger sulphonic group domains and clearer nano-phase separated structures than that of SPEEK. The main-chain-type and side-chain-type membranes revealed excellent nano-phase separated structures, indicating that the flexibility of the side-chain-type sulphonic acid groups played an important role on membrane morphology to allow for the formation of a well-defined morphology.

3.3. Thermal characteristics

The thermal stability of the MS-SPEEKs was investigated by TGA. Fig. 4 shows the 5% (w/w) loss temperature (T_{d5}) of the MS-SPEEKs. PEEK is a thermally stable polymer and possesses a T_{d5} of 581 °C. In contrast, the MS-SPEEKs displayed two weight loss steps and a lower T_{d5} than that of PEEK. The first weight loss step was assigned to the loss of $-\text{SO}_3\text{H}$ groups from the main chain and side chain of the polymer due to the evolution of SO and SO_2 . The second step was attributed to the degradation of the main polymer chain. Thus, the results indicated that the degradation of MS-SPEEK began with the desulphonation of sulphonic acid groups. The value of T_{d5} increased with an increase in the number of pendant sulphonated side chain groups. In particular, MS47, MS52, MS57, MS62 and MS70 presented a T_{d5} of 382 °C, 389 °C, 398 °C, 406 °C and 413 °C, respectively.

Differential scanning calorimetry (DSC) was conducted to characterise the thermal transition of the MS-SPEEKs. As shown in Fig. 5, the DSC traces increased with an increase in the DS due to the interaction of main-chain-type sulphonic acid groups with side-chain-type sulphonic acid groups. Namely, the T_g of MS47, MS52, MS57, MS62 and MS70 was 263 °C, 268 °C, 273 °C, 277 °C and 285 °C, respectively,

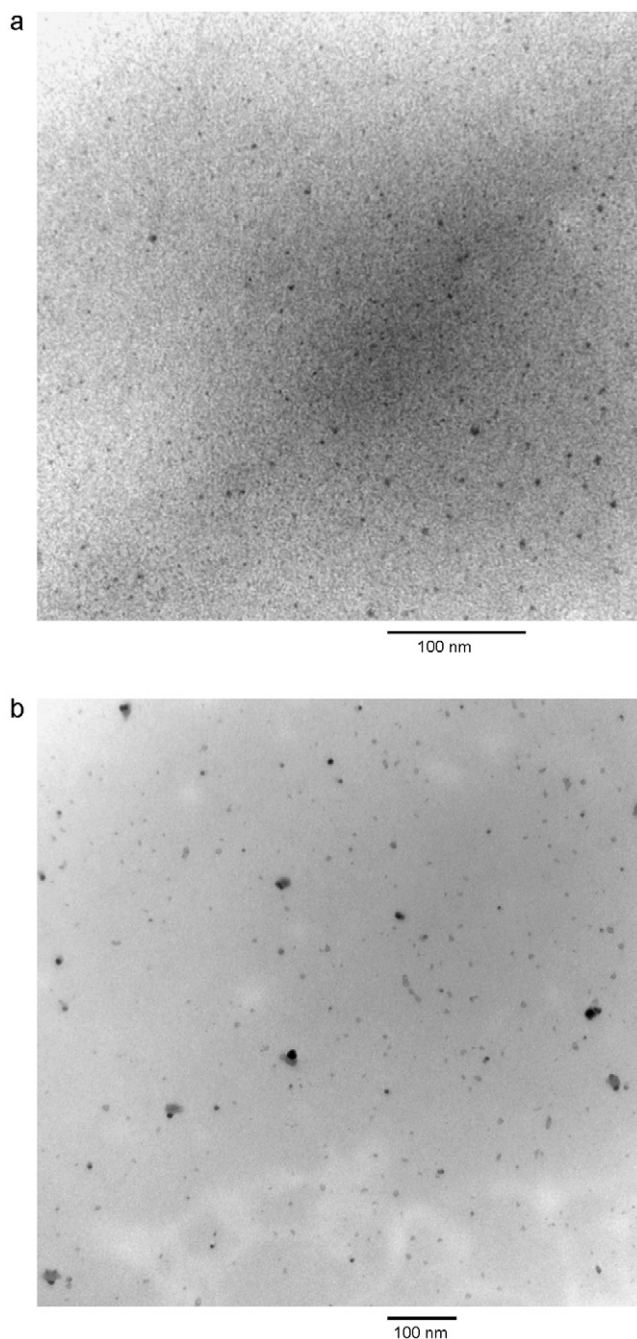


Fig. 3. The TEM images of (a) SPEEK (300,000×) and (b) MS-SPEEK (150,000×).

3.4. Liquid uptake

The proton conductivity and mechanical properties of a membrane are strongly related to the liquid content. Liquid within the membrane acts a carrier for proton transportation and maintains high proton conductivity. However, excessive liquid uptake in a membrane results in mechanical instability, which leads to weakness or dimensional mismatch upon incorporation into a membrane electrode assembly. In general, the liquid uptake of highly sulphonated main-chain-type poly(arylene ether)s increases dramatically at the threshold temperature, which results in disintegrated morphology. One way to improve the nano-phase separated morphology is to separate the hydrophilic sulphonic acid domain from the hydrophobic main chain domain by introducing sulphonic acid groups on the side chains.

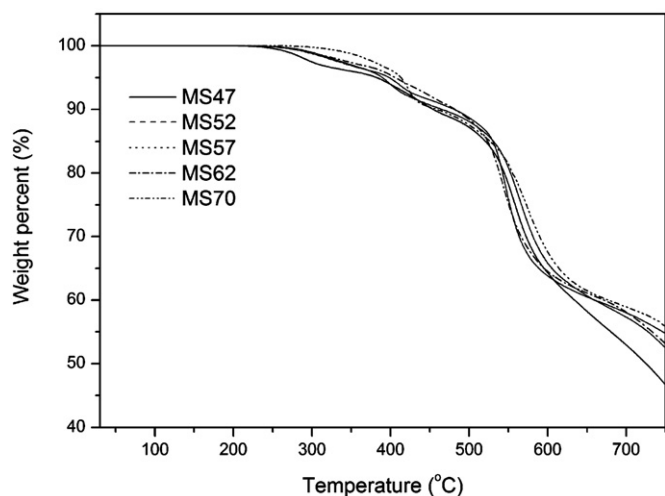


Fig. 4. The thermogravimetric curves of MS-SPEEKs.

Fig. 6 shows a plot of the liquid uptake of MS-SPEEK membranes versus the temperature and methanol concentration (2 M). At 30 °C, the water uptake of MS-SPEEK membranes increased from 15% to 30% as the DS increased and the methanol uptake was almost the same with water uptake. Moreover, the liquid uptake of the membranes increased with an increase in temperature and methanol concentration. When the temperature was 80 °C, the mobility of the polymer chain, free volume available for liquid absorption and plastic effect of methanol was increased. As the DS increased and the threshold temperature was exceeded, the membranes dramatically swelled, disintegrating the nano-phase separated morphology. High degree of sulphonated membranes presented a threshold temperature of approximately 60 °C. For MS62 and MS70, the liquid uptake increased to 51% and 78% at 80 °C in water, while for MS57, MS62 and MS70, the liquid uptake dramatically increased to 128%, 220% and 310% in methanol solution, respectively. MS47, MS52 showed moderate liquid uptake values of 20% and 25% in water, while 26% and 37% in methanol solution, respectively, ensuring good hydrolytic stability at methanol solution and high temperature. Thus, the introduction of side-chain-type sulphonic acid groups allowed for the formation of a well-defined morphology. Liquid molecules were restricted to the

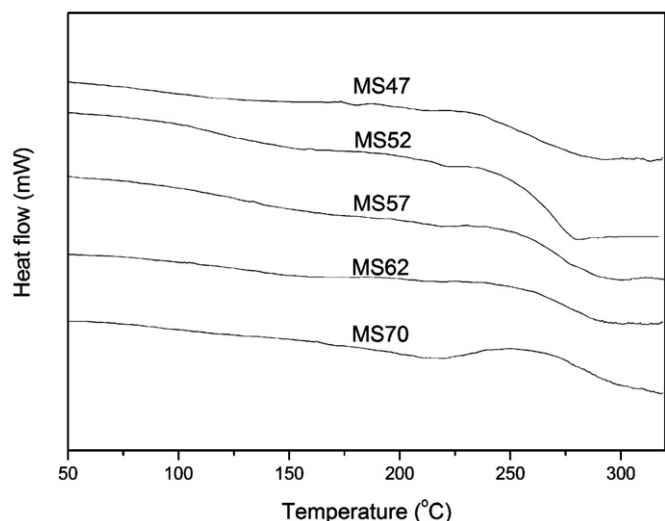


Fig. 5. The transition temperature of MS-SPEEKs.

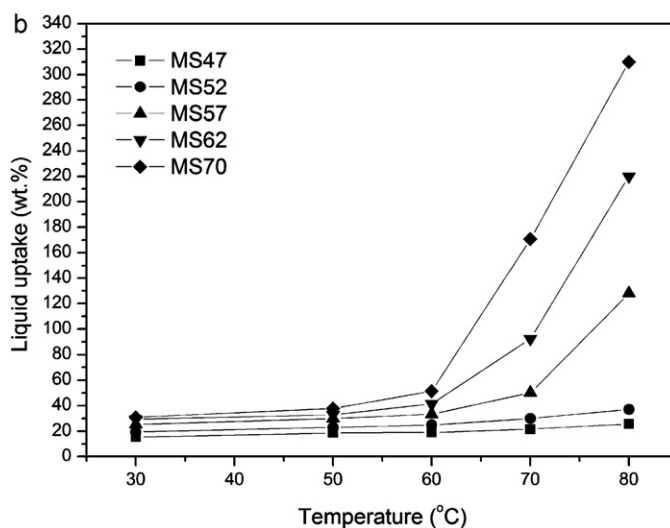
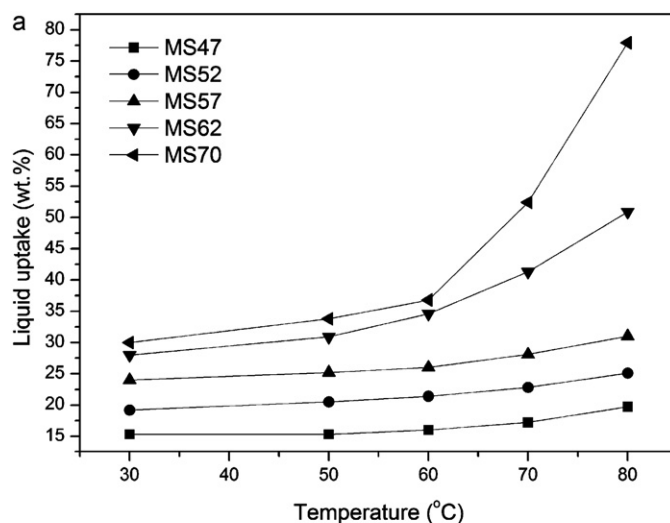


Fig. 6. The liquid uptake of MS-SPEEKs under (a) water and (b) 2 M methanol solution.

hydrophilic domain of the membranes and were separated from the hydrophobic domain, which suppressed excessive uptake.

3.5. Methanol permeability

Membranes used in DMFCs must possess high proton conductivity and be an effective barrier for methanol crossover from the anode to the cathode compartment. Fig. 7 shows the methanol permeability of MS-SPEEKs. As the DS and liquid uptake increased, the methanol permeability of MS-SPEEK membranes increased from $8.83 \times 10^{-8} \text{ cm}^2 \text{ s}^{-1}$ to $3.31 \times 10^{-7} \text{ cm}^2 \text{ s}^{-1}$ at 30 °C, which is significantly lower than that of the Nafion® 117 membrane ($2 \times 10^{-6} \text{ cm}^2 \text{ s}^{-1}$). Due to their low liquid uptake values at 30 °C, the methanol permeability of MS47, MS52, MS57, MS62 and MS70 was $8.83 \times 10^{-8} \text{ cm}^2 \text{ s}^{-1}$, $1.04 \times 10^{-7} \text{ cm}^2 \text{ s}^{-1}$, $1.87 \times 10^{-7} \text{ cm}^2 \text{ s}^{-1}$, $2.66 \times 10^{-7} \text{ cm}^2 \text{ s}^{-1}$ and $3.31 \times 10^{-7} \text{ cm}^2 \text{ s}^{-1}$, respectively. When the temperature increased to 80 °C, the methanol permeability of MS47, MS52, MS57, MS62 and MS70 was $1.24 \times 10^{-6} \text{ cm}^2 \text{ s}^{-1}$, $3.26 \times 10^{-6} \text{ cm}^2 \text{ s}^{-1}$, $5.78 \times 10^{-6} \text{ cm}^2 \text{ s}^{-1}$, $7.52 \times 10^{-6} \text{ cm}^2 \text{ s}^{-1}$ and $1.13 \times 10^{-5} \text{ cm}^2 \text{ s}^{-1}$, respectively. As shown in Fig. 7, for a fully hydrated membrane, methanol transport is dependent on the DS and liquid uptake at various temperatures because methanol permeates through hydrophilic domains, which consist of sulphonic

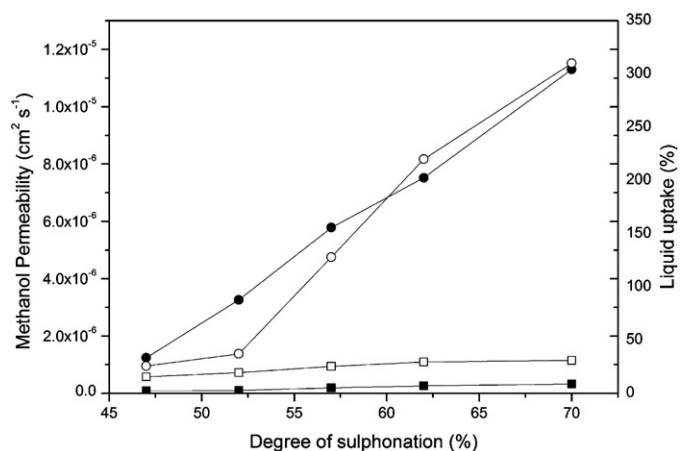


Fig. 7. The methanol permeability of MS-SPEEKs: Methanol permeability: (■) 30 °C and (●) 80 °C. (b) Liquid uptake: (□) 30 °C and (○) 80 °C.

acid groups. As a result, the hydrophilic domains increased with an increase in the DS and liquid uptake.

3.6. Proton conductivity

Non-fluorinated sulphonated polymers require high DS values to attain high proton conductivity due to the lower acidity of sulphonic acid groups, flexibility, and nano-phase separation compared to Nafion®. In general, conductivities greater than $10^{-2} \text{ S cm}^{-1}$ are required for PEMs in fuel cells. Fig. 8 shows the proton conductivity of MS-SPEEK membranes as a function of the temperature and methanol solution. The proton conductivity of PEMs increases with an increase in the sulphonic group content, temperature and liquid uptake due to the diffusion and thermal motion of protons in the ion networks of membranes. As shown in Fig. 8(a), the proton conductivity of MS-SPEEK membranes at 30–80 °C increased to $0.013\text{--}0.029 \text{ S cm}^{-1}$ for MS47, $0.031\text{--}0.121 \text{ S cm}^{-1}$ for MS52, $0.052\text{--}0.142 \text{ S cm}^{-1}$ for MS57, $0.067\text{--}0.166 \text{ S cm}^{-1}$ for MS62 and to $0.077\text{--}0.182 \text{ S cm}^{-1}$ for MS70. Thus, the addition of side-chain-type sulphonic acid groups increased the proton conductivity of the material. As shown in Fig. 8(b), because of the plastic effect of methanol the proton conductivity of MS-SPEEK membranes at 30–80 °C increased to $0.014\text{--}0.032 \text{ S cm}^{-1}$ for MS47, $0.038\text{--}0.131 \text{ S cm}^{-1}$ for MS52, $0.057\text{--}0.174 \text{ S cm}^{-1}$ for MS57, $0.072\text{--}0.194 \text{ S cm}^{-1}$ for MS62 and to $0.091\text{--}0.218 \text{ S cm}^{-1}$ for MS70.

For pristine SPEEK membranes, hydrophilic sulphonic acid groups may aggregate into hydrophilic ionic clusters, which are dispersed throughout the hydrophobic polymer domain. Hydrophilic ionic clusters were isolated in the continuous hydrophobic domain; however, the incorporation of side-chain-type sulphonic acid groups improved the aggregation of ionic clusters, which enhanced nano-phase separation as shown in TEM images. As the number of sulphonic acid groups increased, ion networks with good connectivity were produced, through which protons can be rapidly transported.

From the results of proton conductivity and methanol permeability, we could calculate the selectivity parameter to directly compare the applicability for DMFCs between the membranes. The higher the selectivity value, the better the membrane performance is. Fig. 9 shows the selectivity parameters of MS-SPEEKs at 80 °C. The membranes showed an optimal selectivity value of MS52 and then decreasing with the increase of DS. This result suggested that the MS-SPEEKs have more impact on the reduction of methanol permeability than that of proton conductivity.

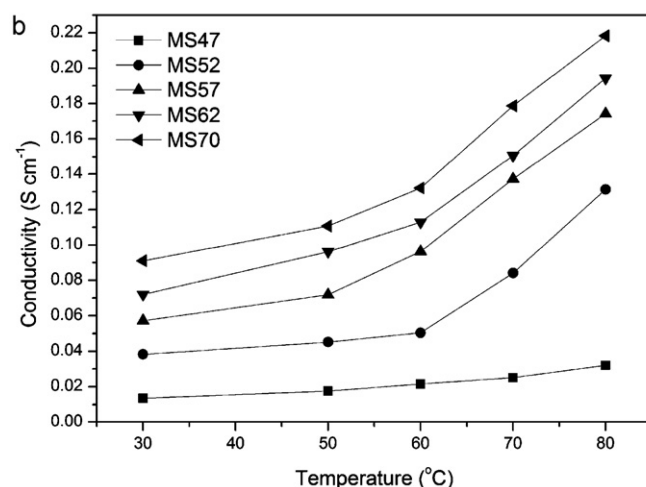
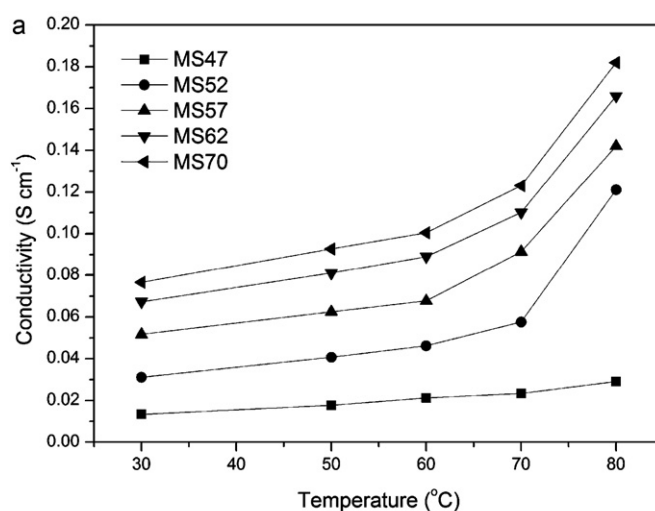


Fig. 8. The proton conductivity for MS-SPEEKs in (a) water and (b) 2M methanol solution.

3.7. Electro-osmotic drag coefficient

Water transportation is critical role for optimal cell performance in DMFC. The transport of water can occur by different mechanisms, such as water transport across the membrane via water activity

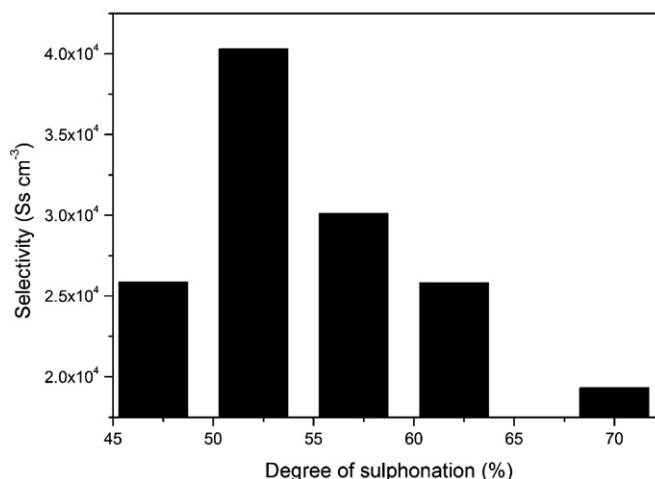


Fig. 9. The selectivity parameters of MS-SPEEKs at 80 °C.

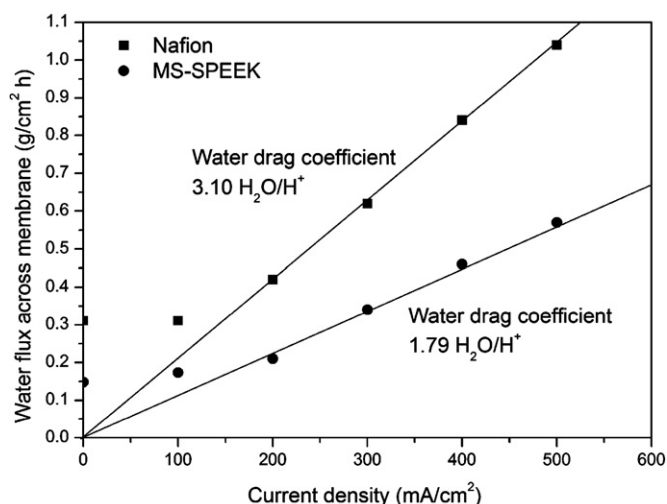


Fig. 10. Water flux across Nafion® 117 and MS-SPEEK under DMFC single-cell test at 80 °C.

gradients, electro-osmotic drag by the protons migrating from the anode to cathode side and by hydraulic pressure gradients across the membrane.

Fig. 10 shows the water flux across membrane of Nafion® 117® and MS-SPEEK as a function of current density at 80 °C. At open circuit voltage (OCV) condition, the water flux across the membrane was exclusively diffusive due to the water activity gradient between the anode and cathode side. The water flux across MS-SPEEK at OCV was noticeably lower than that of Nafion® 117®, even though the membrane thickness of MS-SPEEK was thinner than Nafion® 117®. When the cell under current, both electro-osmosis and diffusion of water can contribute from anode to cathode. Fortunately, that at a sufficiently high current density and high levels of cathode humidification can eliminate diffusive transport, and water flux is driven exclusively by electro-osmotic drag. The electro-osmotic drag coefficient of water can be calculated from the slope of the straight line that crossing the origin in the plot. Fig. 10 shows that the electro-osmotic drag coefficient of MS-SPEEK was lower than that of Nafion® 117®. The lower water diffusivity, methanol permeability, and electro-osmotic drag coefficient for MS-SPEEK indicated that MS-SPEEK is a promising candidate for DMFC applications.

3.8. Single-cell performance

Nafion® 117 and MS-SPEEK membranes were tested in a DMFC single cell. Fig. 11(a) and (b) shows the performance results of various MS-SPEEKs at 60 °C and 80 °C, including the polarisation and power density as a function of the current density. All of the characteristic curves displayed similar polarisation behaviour. In the region of low current density, activation control caused a large drop in potential, which further decreased at intermediate current densities due to the intrinsic ohmic resistance. Although these factors contribute to a lower output upon application of a load to the system, only methanol crossover actively decreases the open circuit voltage (OCV). Nafion® 117 has a thickness of ~178 μm, whereas the thickness of the MS-SPEEK membranes was approximately ~65 μm. In theory, Nafion® 117 is preferred in DMFCs because thicker membranes assure limited methanol crossover. However, as shown in Fig. 11, single cells prepared with MS47 and MS52 membranes exhibited higher OCVs (0.868 V and 0.830 V) than that of Nafion® 117 (0.803 V) with 2 M methanol at 80 °C. This result clearly indicates that the introduction of pendent side-chain-type sulphonic acid groups significantly decreased

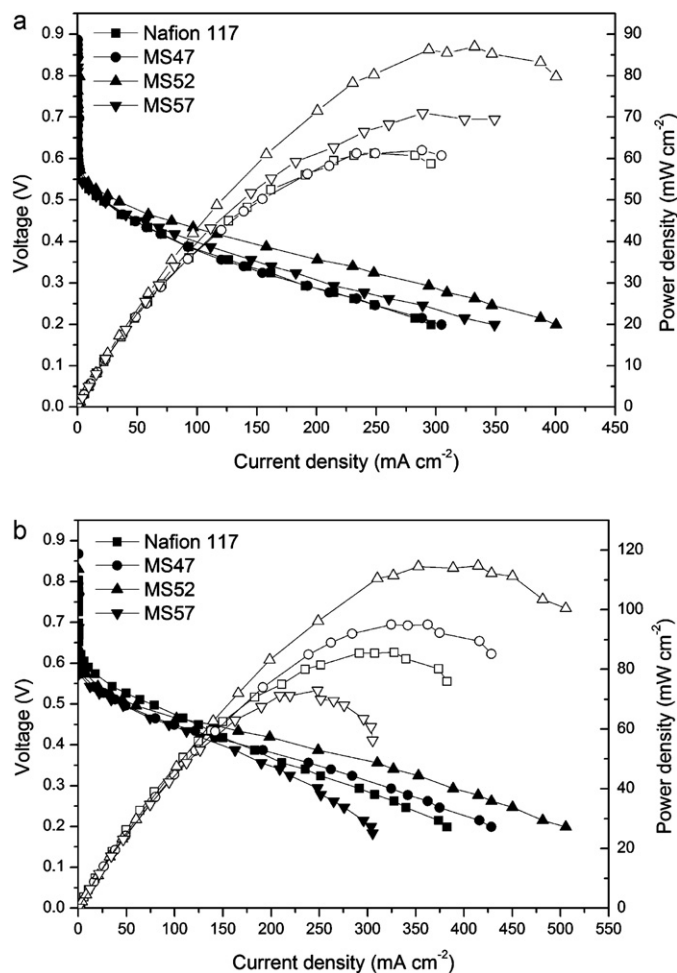


Fig. 11. The performance curves of Nafion® 117 and MS-SPEEKs at (a) 60 °C and (b) 80 °C.

the rate of methanol crossover in DMFCs due to the relatively low methanol permeability of the membrane. Although the conductivity of MS-SPEEK membranes was lower than that of Nafion®, the DMFC performance was improved due to the reduction in methanol crossover and membrane thickness. As shown in Fig. 11, as the DS increased, the performance of MS57 increased from 70 to 73 mW cm⁻² at 60–80 °C due to high methanol uptake, low mechanical properties and selectivity at high DS and temperature. Similar to Nafion® 117, the cell performance of MS47 increased from 61 to 95 mW cm⁻² at 60–80 °C. The MS52 membrane had the highest power density of 86–115 mW cm⁻² at 60–80 °C, which was greater than that of the other MS-SPEEKs and Nafion® 117 (61–86 mW cm⁻²). The introduction of pendent side-chain-type sulphonic acid groups significantly increased single-cell performance by more than approximately 20% at 80 °C, indicating that MS-SPEEK is a promising candidate for DMFCs.

4. Conclusion

Novel MS-SPEEKs were synthesised to improve the nano-phase separated morphology of pristine SPEEKs. The ¹H NMR spectroscopy results revealed that the ratio of main-chain-type sulphonic acid groups to side-chain-type sulphonic acid groups was equal to 1:1. The introduction of side-chain-type sulphonic acid groups allowed for the formation of a well-defined nano-phase separated morphology. As a result, water molecules were restricted to the hydrophilic domain of the membrane and were

separated from the hydrophobic domain, which suppressed excessive water uptake and methanol permeability. The experimental results revealed that the MS52 membrane exhibited higher OCV and superior single-cell performance compared to other MS-SPEEKs and Nafion® 117. The promising single-cell performance results observed in the present study suggest that MS-SPEEKs with improved nano-phase separation may improve DMFC applications.

Acknowledgements

The authors are extremely grateful to Ms P.Y. Lin and Professor W.H. Lai for their crucial contribution to the ¹H NMR experiments and the single-cell performance test.

References

- [1] V. Neburchilov, J. Martin, H. Wang, J. Zhang, J. Power Sources 169 (2007) 221–238.
- [2] M.A. Hickner, H. Ghassemi, Y.S. Kim, B.R. Einsla, J.E. McGrath, Chem. Rev. 104 (2004) 4587–4612.
- [3] D.R. Vernon, F. Meng, S.F. Dec, D.L. Williamson, J.A. Turner, A.M. Herring, J. Power Sources 139 (2005) 141–151.
- [4] S. Tan, D. Belanger, J. Phys. Chem. B 109 (2005) 23480–23490.
- [5] R. Wycisk, J. Chisholm, J. Lee, J. Lin, P.N. Pintauro, J. Power Sources 163 (2006) 9–17.
- [6] J. Lin, J.K. Lee, M. Kellner, R. Wycisk, P.N. Pintauro, J. Electrochem. Soc. 153 (2006) A1325–A1331.
- [7] S.M.J. Zaidi, S.D. Mikhailenko, G.P. Robertson, M.D. Guiver, S. Kaliaguine, J. Membr. Sci. 173 (2000) 17–34.
- [8] A. Carbone, R. Pedicini, G. Portale, A. Longo, L. D'Ilario, E. Passalacqua, J. Power Sources 163 (2006) 18–26.
- [9] P. Xing, G.P. Robertson, M.D. Guiver, S.D. Mikhailenko, S. Kaliaguine, Macromolecules 37 (2004) 7960–7967.
- [10] P. Xing, G.P. Robertson, M.D. Guiver, S.D. Mikhailenko, S. Kaliaguine, J. Polym. Sci. A: Polym. Chem. 42 (2004) 2866–2876.
- [11] K. Miyatake, Y. Chikashige, M. Watanabe, Macromolecules 36 (2003) 9691–9693.
- [12] H.S. Lee, A.S. Badami, A. Roy, J.E. McGrath, J. Polym. Sci. Part A: Polym. Chem. 45 (2007) 4879–4890.
- [13] J.C. Tsai, J.F. Kuo, C.Y. Chen, J. Power Sources 174 (2007) 103–113.
- [14] W. Essafi, G. Gebel, R. Mercier, Macromolecules 37 (2004) 1431–1440.
- [15] N. Asano, M. Aoki, S. Suzuki, K. Miyatake, H. Uchida, M. Watanabe, J. Am. Chem. Soc. 128 (2006) 1762–1769.
- [16] J. Jouanneau, R. Mercier, L. Gomom, G. Gebel, Macromolecules 40 (2007) 983–990.
- [17] D.J. Jones, J.J. Roziere, J. Membr. Sci. 185 (2001) 41–58.
- [18] C. Manea, M. Mulder, J. Membr. Sci. 206 (2002) 443–453.
- [19] K.D. Kreuer, J. Membr. Sci. 185 (2001) 29–39.
- [20] P. Jannasch, Fuel Cells 5 (2005) 248–260.
- [21] B. Lafitte, M. Puchner, P. Jannasch, Macromol. Rapid Commun. 26 (2005) 1464–1468.
- [22] B. Lafitte, P. Jannasch, Adv. Funct. Mater. 17 (2007) 2823–2834.
- [23] E.P. Jutemar, P. Jannasch, J. Membr. Sci. 351 (2010) 87–95.
- [24] Y. Yin, Y. Suto, T. Sakabe, S. Chen, S. Hayashi, T. Mishima, O. Yamada, K. Tanaka, H. Kita, K. Okamoto, Macromolecules 39 (2006) 1189–1198.
- [25] Z. Hu, Y. Yin, K. Okamoto, Y. Moriyama, A. Morikawa, J. Membr. Sci. 329 (2009) 146–152.
- [26] Y. Yin, Q. Du, Y. Qin, Y. Zhou, K. Okamoto, J. Membr. Sci. 367 (2011) 211–219.
- [27] T. Yasuda, Y. Li, K. Miyatake, M. Hirai, M. Nanasawa, M. Watanabe, J. Polym. Sci. Part A: Polym. Chem. 44 (2006) 3995–4005.
- [28] K. Miyatake, T. Yasuda, M. Hirai, M. Nanasawa, M. Watanabe, J. Polym. Sci. Part A: Polym. Chem. 45 (2007) 157–163.
- [29] A. Kabasawa, J. Saito, H. Yano, K. Miyatake, H. Uchida, M. Watanabe, Electrochim. Acta 54 (2009) 1076–1082.
- [30] D.S. Kim, G.P. Robertson, M.D. Guiver, Macromolecules 41 (2008) 2126–2134.
- [31] D.S. Kim, Y.S. Kim, M.D. Guiver, J. Ding, B.S. Pivovar, J. Power Sources 182 (2008) 100–105.
- [32] B. Liu, Y.S. Kim, W. Hu, G.P. Robertson, B.S. Pivovar, M.D. Guiver, J. Power Sources 185 (2008) 899–903.
- [33] Y. Zhang, Y. Wan, C. Zhao, K. Shao, G. Zhang, H. Li, H. Lin, H. Na, Polymer 50 (2009) 4471–4478.
- [34] J. Zhu, K. Shao, G. Zhang, C. Zhao, Y. Zhang, H. Li, M. Han, H. Lin, D. Xu, H. Yu, H. Na, Polymer 51 (2010) 3047–3053.
- [35] Y. Zhang, G. Zhang, Y. Wan, C. Zhao, K. Shao, H. Li, M. Han, J. Zhu, S. Xu, Z. Liu, H. Na, J. Polym. Sci. Part A: Polym. Chem. 48 (2010) 5824–5832.
- [36] H. Zhang, X. Fan, J. Zhang, Z. Zhou, Solid State Ionics 179 (2008) 1409–1412.
- [37] Y.S. Kim, M.J. Sumner, W.L. Harrison, J.S. Riffle, J.E. McGrath, B.S. Pivovar, J. Electrochem. Soc. 151 (2004) A2150–A2156.
- [38] X. Ren, W. Henderson, S. Gottesfeld, J. Electrochem. Soc. 144 (1997) L267–L270.
- [39] P. Xing, G.P. Robertson, M.D. Guiver, S.D. Mikhailenko, K. Wang, S. Kaliaguine, J. Membr. Sci. 229 (2004) 95–106.